Appl. Phys. A 79, 1349–1352 (2004)
DOI: 10.1007/s00339-004-2776-x

Applied Physics A
Materials Science & Processing

Laser synthesis of new materials

W.D. SONG[1,✉]
M.H. HONG[1]
T. OSIPOWICZ[2]
D.Y. DAI[1]
S.I. PANG[1]
Y.Z. PENG[1]
J.F. CHONG[1]
C.W. AN[1]
Y.F. LIEW[1]
T.C. CHONG[1]

[1] Data Storage Institute, Agency of Science, Technology and Research, DSI Building 5, Engineering Drive 1 (off Kent Ridge Crescent, NUS), Singapore 117608
[2] National University of Singapore, Kent Ridge Crescent, Singapore 119260

Received: 15 September 2003/Accepted: 4 March 2004

ABSTRACT The dual-beam laser ablation of different targets for synthesizing new materials within the overlapping plasma area has been investigated. This method is termed ‘laser synthesis of new materials’ and it is flexible in tuning the composition of the new materials by varying the targets, the laser fluence on each target and the input gas as well as the substrate position within the overlapping plasma area. A new Ba–Fe–Y–O magnetic material has been synthesized by this method, which can be written as $BaO_kFe_{2-x}Y_xO_3$, where k is either 6 or 11 and x is about 0.4 or 0.9 for $BaFe_{9.2}Y_{2.6}O_{20}$ or $BaFe_{12.3}Y_{9.6}O_{33.3}$ material. Both materials are permanent magnets and have hexagonal structure. The lattice parameters a and c are 0.551 nm and 2.337 nm for $BaFe_{9.2}Y_{2.6}O_{20}$ and 0.747 nm and 2.332 nm for $BaFe_{12.3}Y_{9.6}O_{33.3}$, respectively.

PACS 81.20.-n; 81.15.Fg; 75.50.Vv

1 Introduction

Based on laser ablation of YBa_2O_x and CuO targets by an Nd : YAG laser and a KrF excimer laser, Hussey and Gupta [1] successfully synthesized $YBa_2Cu_3O_{7-x}$ superconductor thin films. They found that no additional phases were detected in the films. Nevertheless, the formation of small amounts of secondary phases cannot be completely ruled out. Latterly, Ong et al. developed their dual-beam pulsed laser deposition system for doping impurity into the thin films to improve the film properties [2, 3].

Recently, we found that this method may not only be used to synthesize a known material [1] or dope impurity into the films [2, 3], but also to synthesize new materials. In this article, we report two laser beams split from an excimer laser to ablate barium ferrite ($BaFe_{12}O_{19}$) and yttrium oxide (Y_2O_3) targets for synthesis of new materials.

2 Experimental

The schematic diagram of our laser synthesis system is shown in Fig. 1. A KrF excimer laser (248 nm, 30 ns) beam was split into two beams, which were focused onto the rotating barium ferrite ($BaFe_{12}O_{19}$) and yttrium oxide (Y_2O_3) targets with two focusing lenses to produce two plumes, respectively. The distance between the two laser beams on the targets is about 2 cm. The laser fluence on each target is about 2.5 J/cm^2. Actually, it can be easily changed by moving the lens position or varying the laser energy. The targets were mounted at 45° with respect to the laser beams. The distance between the two target centers is 3.5 cm. Facing the targets at a distance of 4.5 cm, a group of (001) single-crystal Al_2O_3 substrates with a typical size of 5×10 mm^2 was mounted on a two-inch stainless steel holder by silver paste. A background pressure of 10^{-5} Torr was achieved with a turbomolecular pump. During the synthesis, an oxygen pressure of 50 mTorr was maintained and the substrates were heated to 900 °C. The synthesized materials were typically grown for 12 000 pulses at a repetition rate of 10 Hz. After laser synthesis, the materials were cooled to room temperature in an atmosphere of pure oxygen.

We term this dual-beam laser ablation of different targets for synthesizing new materials within the overlapping plasma area ‘laser synthesis of new materials’. It has following features. The components including atoms, molecules, electrons, ions and clusters for material synthesis are high-

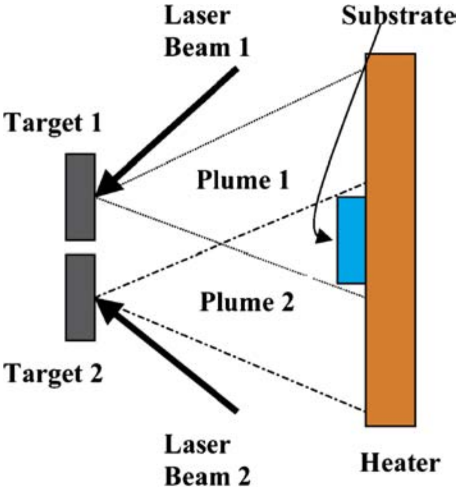

FIGURE 1 The schematic diagram of the laser synthesis system

✉ Fax: +65-67771349, E-mail: song_wendong@dsi.a-star.edu.sg

energetic evaporants generated by laser ablation [4]. The use of short laser pulses for ablation is more likely to achieve congruent ablation to preserve stoichiometry during mass transfer from target to substrate [5], which makes the composition of the new materials easily controlled. Since laser interaction with gas-phase species is relatively weak [6], many kinds of reactive gases can be input for material synthesis. It is flexible in tuning synthesized elements and compositions by varying the targets, the laser fluence on each target and the input gas as well as the substrate position within the overlapping plasma area. A preferred single-crystal substrate can be chosen to lead to crystal growth of new materials. It can also heat the substrate to high temperature to provide an appropriate environment for new-material synthesis. The method is inexpensive, simple and fast to synthesize new materials.

3 Results and discussion

According to the above experimental conditions, a group of samples was prepared by the laser synthesis system. The composition of Ba–Fe–Y–O materials is analyzed by Rutherford backscattering spectrometry (RBS). Figure 2 shows the RBS spectra of two typical Ba–Fe–Y–O materials on single-crystal Al_2O_3 substrates. Analysis of the RBS data of the Ba–Fe–Y–O materials yields the composition of $BaFe_{12.3}Y_{9.6}O_{33.3}$ for the sample in the face of the Y_2O_3 target center and $BaFe_{9.2}Y_{2.6}O_{20}$ for the sample in the face of the $BaFe_{12}O_{19}$ target center. The thickness is 1.76×10^{18} atoms/cm^2 ($\sim 0.41\,\mu m$) for $BaFe_{12.3}Y_{9.6}O_{33.3}$ material on the substrate and 1.73×10^{18} atoms/cm^2 ($\sim 0.38\,\mu m$) for $BaFe_{9.2}Y_{2.6}O_{20}$ material on the substrate, respectively. It is well known that $BaFe_{12}O_{19}$ can be written as $BaO_kFe_2O_3$, where k is equal to 6 [7]. Considering the compositional accuracy within a few percent for RBS [8], we can conclude that $BaFe_{9.2}Y_{2.6}O_{20}$ material has a composition of $BaO_kFe_{2-x}Y_xO_3$, where k and x are 6 and 0.4, respectively. $BaFe_{12.3}Y_{9.6}O_{33.3}$ material has a composition of $BaO_kFe_{2-x}Y_xO_3$, where k and x are 11 and 0.9, respectively. For the above materials, they have the composition of $BaO_kFe_{2-x}Y_xO_3$ by element replacement of Y to Fe and k depends on the element replacement ratio of Y to Fe.

Figure 3 shows the Raman spectra of $BaFe_{12.3}Y_{9.6}O_{33.3}$ and $BaFe_{9.2}Y_{2.6}O_{20}$ materials as well as Y_2O_3 and $BaFe_{12}O_{19}$ targets. Comparing the four Raman spectra, it is found that both Raman spectra of $BaFe_{12.3}Y_{9.6}O_{33.3}$ and $BaFe_{9.2}Y_{2.6}O_{20}$ materials are similar to the $BaFe_{12}O_{19}$ target and different from the Y_2O_3 target. Based on D_{6h} symmetry of barium ferrite crystals, 42 Raman-active modes ($11A_{1g}+14E_{1g}+17E_{2g}$) are expected [9, 10]. The A_{1g} modes at 317 cm^{-1}, 411 cm^{-1}, 470 cm^{-1}, 614 cm^{-1}, 686 cm^{-1} and 713 cm^{-1}, E_{1g} modes at 184 cm^{-1}, 212 cm^{-1} and 286 cm^{-1} and E_{2g} modes at 337 cm^{-1} and 529 cm^{-1} are observed in the Raman spectrum of the $BaFe_{12}O_{19}$ (BaM) target. These Raman modes were also found in the Raman spectra of the synthesized $BaFe_{12.3}Y_{9.6}O_{33.3}$ and $BaFe_{9.2}Y_{2.6}O_{20}$ materials. In addition, a peak at 494 cm^{-1} and a weak peak at 244 cm^{-1} were observed in the Raman spectrum of $BaFe_{12.3}Y_{9.6}O_{33.3}$ material, which did not belong to the BaM phase [9] or the yttrium oxide phase. This indicates that an additional phase may exist in the $BaFe_{12.3}Y_{9.6}O_{33.3}$ material, which is identified as Raman-active modes of α-Fe_2O_3 [9].

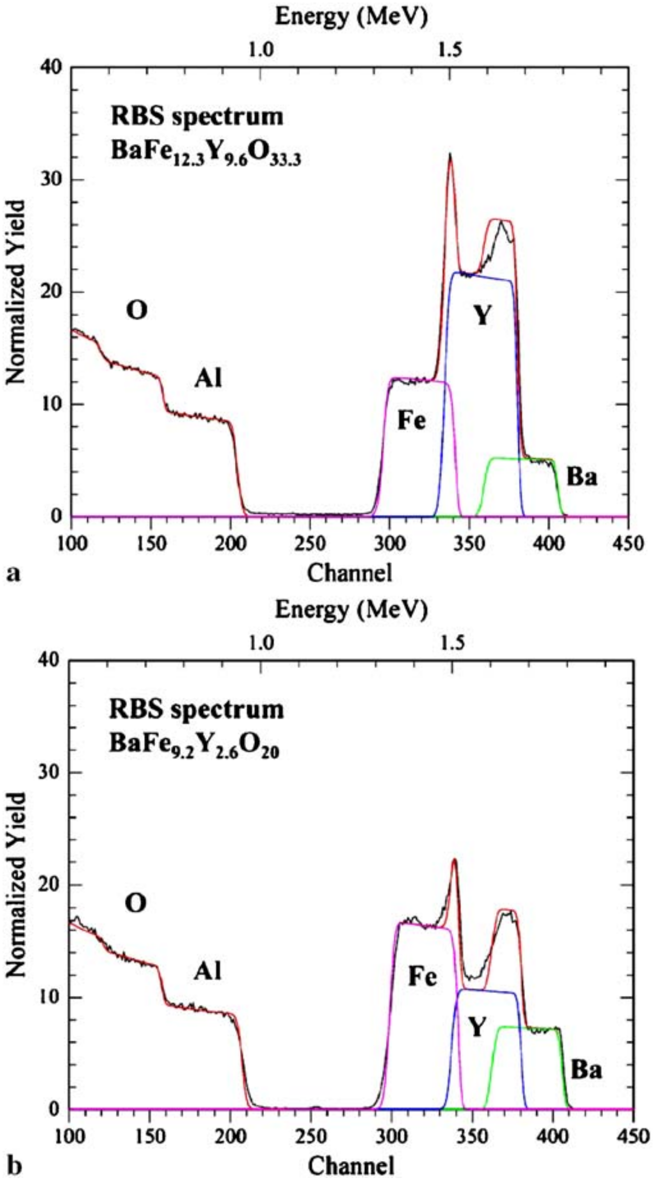

FIGURE 2 The RBS spectra of $BaFe_{12.3}Y_{9.6}O_{33.3}$ and $BaFe_{9.2}Y_{2.6}O_{20}$ materials on single-crystal Al_2O_3 substrates

Based on the RBS and Raman-spectra analysis above, it is reasonable to consider both $BaFe_{12.3}Y_{9.6}O_{33.3}$ and $BaFe_{9.2}Y_{2.6}O_{20}$ as having a hexagonal structure like $BaFe_{12}O_{19}$. The crystal structure of the two materials is further characterized by X-ray diffractometry (XRD) and transmission electron microscopy (TEM). Figure 4 shows the XRD data and selected area diffraction patterns of the $BaFe_{12.3}Y_{9.6}O_{33.3}$ and $BaFe_{9.2}Y_{2.6}O_{20}$ materials on the single-crystal Al_2O_3 substrates. The diffraction patterns in the inset of Fig. 4 indicate that both synthesized $BaFe_{12.3}Y_{9.6}O_{33.3}$ and $BaFe_{9.2}Y_{2.6}O_{20}$ materials have hexagonal structure, which is consistent with RBS and Raman-spectra analysis. Combining Bragg's law and the plane-spacing equation for the hexagonal structure [11] yields $\sin^2\theta = A(h^2+hk+k^2)+Cl^2$, where h, k and l are the Miller–Bravais indices, $A=\lambda^2/3a^2$ and

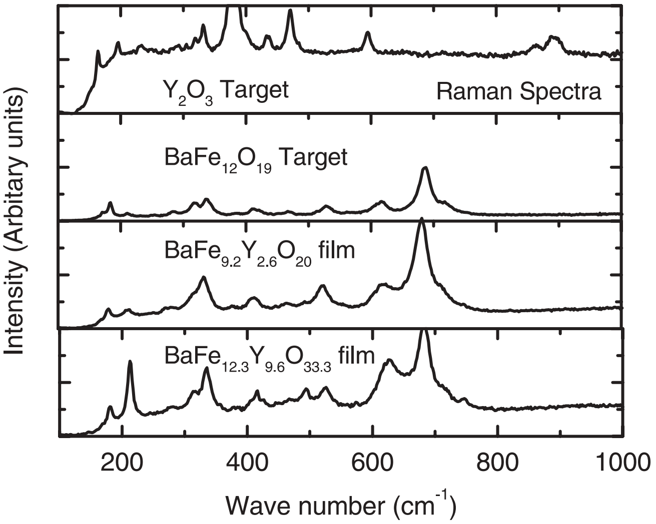

FIGURE 3 The Raman spectra of $BaFe_{12.3}Y_{9.6}O_{33.3}$ and $BaFe_{9.2}Y_{2.6}O_{20}$ materials as well as Y_2O_3 and $BaFe_{12}O_{19}$ targets

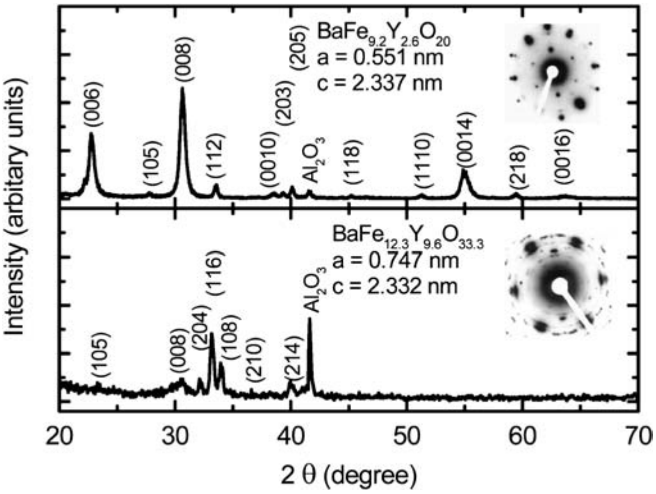

FIGURE 4 The XRD data and selected area diffraction patterns of $BaFe_{12.3}Y_{9.6}O_{33.3}$ and $BaFe_{9.2}Y_{2.6}O_{20}$ materials on single-crystal Al_2O_3 substrates

$C = \lambda^2/3c^2$, θ is the Bragg angle and a and c are lattice parameters of the hexagonal unit cell. According to the structure-factor equation for a hexagonal structure [11], the reflections are absent when $h + 2k = 3N$ (where N is an integer) and l is odd. Following the identification method in the literature [11], XRD peaks can be identified and the lattice parameters can be determined as shown in Fig. 4. Comparing the lattice parameters among $BaFe_{12}O_{19}$, $BaFe_{12.3}Y_{9.6}O_{33.3}$ and $BaFe_{9.2}Y_{2.6}O_{20}$ materials, it is found that the lattice parameter c of $BaFe_{12.3}Y_{9.6}O_{33.3}$ or $BaFe_{9.2}Y_{2.6}O_{20}$ material is 2.332 or 2.337 nm, which is close to 2.32 nm of $BaFe_{12}O_{19}$. The lattice parameter a of $BaFe_{9.2}Y_{2.6}O_{20}$ material is 0.551 nm, while that of $BaFe_{12.3}Y_{9.6}O_{33.3}$ is 0.747 nm ($a = 0.588$ nm for $BaFe_{12}O_{19}$). The difference of the lattice parameter a should be induced by element replacement of Y to Fe.

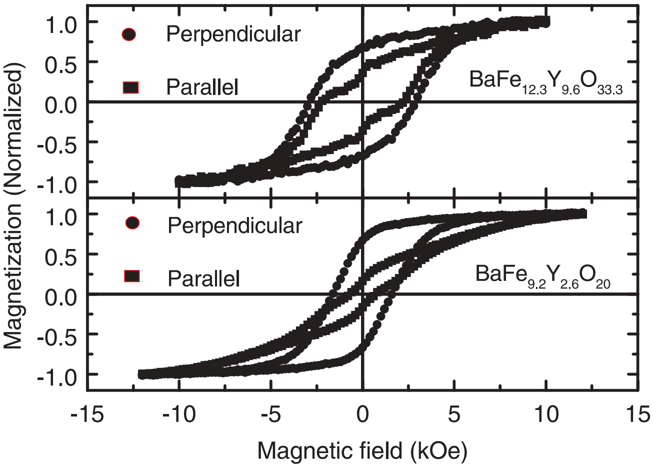

FIGURE 5 The magnetization hysteresis loops of $BaFe_{12.3}Y_{9.6}O_{33.3}$ and $BaFe_{9.2}Y_{2.6}O_{20}$ materials on single-crystal Al_2O_3 substrates

The magnetic properties of the two materials are measured by a vibrating sample magnetometer (VSM). The magnetization hysteresis loops of $BaFe_{12.3}Y_{9.6}O_{33.3}$ and $BaFe_{9.2}Y_{2.6}O_{20}$ materials are shown in Fig. 5. For the synthesized $BaFe_{9.2}Y_{2.6}O_{20}$ material, the perpendicular and in-plane coercivities $H_{c\perp}$ and $H_{c//}$ are 1.6 and 0.7 kOe, respectively. In contrast, for the synthesized $BaFe_{12.3}Y_{9.6}O_{33.3}$ material, the perpendicular coercivity $H_{c\perp}$ and in-plane one $H_{c//}$ are 2.9 and 2.2 kOe, respectively. Therefore, both $BaFe_{12.3}Y_{9.6}O_{33.3}$ and $BaFe_{9.2}Y_{2.6}O_{20}$ materials are permanent magnets or hard magnetic materials, which can be used in recording media, especially perpendicular recording media and microwave devices [12]. For other samples, a similar analysis showed that both the perpendicular and in-plane coercivities increase with element replacement of Y to Fe and reach maximum values at $x \approx 0.9$. At $x > 1$, the coercivities decrease sharply. This indicates that the magnetic properties improve with element replacement of Y to Fe at the atomic ratio of Y to Fe less than 0.9.

4 Conclusion

In summary, a method for laser synthesis of new materials has been investigated. The two laser beams split from an excimer laser were used to ablate barium ferrite ($BaFe_{12}O_{19}$) and yttrium oxide (Y_2O_3) targets to produce two plumes for synthesis of Ba–Fe–Y–O material by element replacement of Y to Fe within the overlapping plasma area. Both $BaFe_{9.2}Y_{2.6}O_{20}$ and $BaFe_{12.3}Y_{9.6}O_{33.3}$ materials can be written as $BaO_kFe_{2-x}Y_xO_3$, where k and x are 6 and 0.4 for $BaFe_{9.2}Y_{2.6}O_{20}$ material and 11 and 0.9 for $BaFe_{12.3}Y_{9.6}O_{33.3}$ material. The synthesized $BaFe_{12.3}Y_{9.6}O_{33.3}$ and $BaFe_{9.2}Y_{2.6}O_{20}$ materials are permanent magnets or hard magnetic materials and have hexagonal structure. The lattice parameters a and c are 0.5509 nm and 2.3374 nm for $BaFe_{9.2}Y_{2.6}O_{20}$ and 0.7474 nm and 2.3323 nm for $BaFe_{12.3}Y_{9.6}O_{33.3}$, respectively. The magnetic properties become better with element replacement of Y to Fe at the atomic ratio of Y to Fe less than 0.9.

REFERENCES

1 B.W. Hussey, A. Gupta: J. Appl. Phys. **72**, 287 (1992)
2 C.K. Ong, S.Y. Xu, W.Z. Zhou: Rev. Sci. Instrum. **69**, 3659 (1998)
3 J. Li, Q. Huang, Z.W. Li, L.P. You, S.Y. Xu, C.K. Ong: J. Appl. Phys. **89**, 7428 (2001)

4 D.B. Geohegan: in *Pulsed Laser Deposition of Thin Films*, ed. by D.B. Chrisey, G.K. Hubler (Wiley-Interscience, New York 1994) pp. 115–162

5 J.T. Cheung: in *Pulsed Laser Deposition of Thin Films*, ed. by D.B. Chrisey, G.K. Hubler (Wiley-Interscience, New York 1994) pp. 1–19

6 T. Venkatesan: in *Pulsed Laser Deposition of Thin Films*, ed. by D.B. Chrisey, G.K. Hubler (Wiley-Interscience, New York 1994) pp. 313–322

7 R.A. McCurrie: *Ferromagnetic Materials* (Academic, London 1994)

8 P.C. Dorsey, S.B. Qadri, K.S. Grabowski, D.L. Knies, P. Lubitz, D.B. Chrisey, J.S. Horwitz: Appl. Phys. Lett. **70**, 1173 (1997)

9 J. Kreisel, S. Pignard, H. Vincent, J.P. Senateur, G. Lucazeau: Appl. Phys. Lett. **73**, 1194 (1998)

10 J. Kreisel, G. Lucazeau, H. Vincent: J. Solid State Chem. **137**, 127 (1998)

11 C. Suryanarayana, M.G. Norton: *X-ray Diffraction* (Plenum, New York, London 1998)

12 C.A. Carosella, D.B. Chrisey, P. Lubitz, J.S. Horwitz, P. Dorsey, R. Seed, C. Vittoria: J. Appl. Phys. **71**, 5107 (1992)